Materials Research Bulletin 47 (2012) 1176–1180

Contents lists available at SciVerse ScienceDirect

Materials Research Bulletin

journal homepage: www.elsevier.com/locate/matresbu

Crystal structure and thermal expansion of $LaCr_{1-x}Mg_xO_3$, $0 < x \leq 0.25$

S.Ya. Istomin *, A.V. Kurlov, S.M. Kazakov, E.V. Antipov

Department of Chemistry, Moscow State University, Leninskie Gory, Moscow 119991, Russia

ARTICLE INFO

Article history:
Received 26 October 2011
Received in revised form 18 January 2012
Accepted 1 February 2012
Available online 10 February 2012

Keywords:
A. Inorganic compounds
A. Oxides
C. X-ray diffraction
D. Crystal structure
D. Thermal expansion

ABSTRACT

Solid solution $LaCr_{1-x}Mg_xO_3$, $0 < x \leq 0.25$ was prepared by heating stoichiometric amounts of appropriate oxides in air at 1400 °C, 48 h. At room temperature it crystallizes in orthorhombically distorted $GdFeO_3$-type structure ($a \approx \sqrt{2} \times a_{per}$; $b \approx \sqrt{2} \times a_{pe}$; $c \approx 2 \times a_{per}$, where a_{per} – perovskite subcell parameter). High-temperature X-ray powder diffraction (HT XRPD) and dilatometry revealed first order phase transition to rhombohedral perovskite phase (R-3c, $a \approx \sqrt{2} \times a_{per}$, $c \approx 2\sqrt{3} \times a_{per}$) at 260–311 °C (OR phase transition). Crystal structures of room-temperature orthorhombic and high-temperature rhombohedral phases for $LaCr_{0.75}Mg_{0.25}O_3$ were refined using HT XRPD data. Temperature of OR phase transition increases gradually with increasing of magnesium content. Low-temperature orthorhombic phase exhibits TEC lower in comparison with high-temperature rhombohedral one (e.g. for $LaCr_{0.85}Mg_{0.15}O_3$ TEC(O) = 8.8 ppm K^{-1}; TEC(R) = 11.6 ppm K^{-1}). TEC for rhombohedral phase increases with increasing magnesium content from 10.4 ppm K^{-1} for $LaCr_{0.95}Mg_{0.05}O_3$ to 12.1 ppm K^{-1} for $LaCr_{0.75}Mg_{0.25}O_3$.

1. Introduction

p-Type doped $LaCrO_3$ is known to be used as interconnect material in solid oxide fuel cells (SOFC) [1]. This is not surprising since $LaCrO_3$ is one of the most thermodynamically stable compounds with high melting point 2783(20) K [2] and high stability in a wide range of $p(O_2)$ [3]. Room temperature modification of $LaCrO_3$ crystallizes in $GdFeO_3$-type structure with unit cell parameters $a \approx \sqrt{2} \times a_{per} = 5.479$ Å; $b \approx \sqrt{2} \times a_{per} = 5.516$ Å; $c \approx 2 \times a_{per} = 7.766$ Å, where a_{per} – perovskite subcell parameter [4]. It undergoes first order phase transition to rhombohedral perovskite (R-3c, $a \approx \sqrt{2} \times a_{per}$, $c \approx 2\sqrt{3} \times a_{per}$) at around 260 °C [5]. Electrical conductivity of undoped $LaCrO_3$ is low and approaches 0.45 S/cm at 900 °C [6]. It can be increased by an appearance of Cr^{4+} cation due to the heterovalent substitution of La^{3+} by Ca^{2+}/Sr^{2+} ($r_{La}{}^{3+} = 1.32$ Å; $r_{Ca}{}^{2+} = 1.35$ Å; $r_{Sr}{}^{2+} = 1.44$ Å, CN = 12 [7]) or Cr^{3+} by Mg^{2+} ($r_{Cr}{}^{3+} = 0.615$ Å; $r_{Mg}{}^{2+} = 0.72$ Å, CN = 6 [7]). Homogeneity range for $La_{1-x}Ca_xCrO_3$ solid solution varies depending on the synthetic conditions used. For example, maximum calcium content approached by the synthesis in air was reported as $x = 0.15$ at 800 °C and $x = 0.31$ at 950 °C [8] or $x = 0.2$, 0.3 and 0.4 at 900 °C, 1000 °C and 1030 °C, respectively, according to ref. [9], and $x = 0.22$ at 1600 °C and $p(O_2) = 10^{-9}$ atm [10]. Even preparation of $x = 0.5$ composition was reported in ref. [11]. At room temperature solid solution $La_{1-x}Ca_xCrO_3$ has $GdFeO_3$-type structure and undergoes phase transformation to rhombohedral perovskite at <327–400 °C depending on x [12]. Homogeneity range for $La_{1-x}Sr_xCrO_3$ seems to be limited to $x \leq 0.3$ [13–15]. There is substantial discrepancy in the literature between the crystal structure data for different compositions. This can be mainly explained by the presence of orthorhombic to rhombohedral (OR) phase transition occurring for this solid solution at around room temperature. Thus, according to [16], OR phase transition takes place at 140 °C for $x = 0.05$, while it shifted to low temperature for $x = 0.13$ (−47 °C) and $x = 0.15$ (−84 °C) [17]. Interest to A-site doped $LaCrO_3$ is still active since the use of various soft-chemistry techniques allows to prepare compounds with new and improved properties [18,19].

$LaCr_{1-x}Mg_xO_3$ was one of the first interconnect materials used in SOFC. It has an advantage over $La_{1-x}M_xCrO_3$, M = Ca, Sr due to weaker dependence of thermal expansion coefficient (TEC) on oxygen partial pressure. For example, TEC of $La_{0.8}Sr_{0.2}CrO_3$ at 1000 °C in hydrogen exceeds TEC in air by 0.3% while for $LaCr_{0.85}Mg_{0.15}O_3$ the difference of 0.1% is observed [1]. However, $LaCr_{1-x}Mg_xO_3$ exhibits lower electrical conductivity in comparison with $La_{1-x}M_xCrO_3$, M = Ca, Sr: at 1000 °C in air 3 S/cm and 14 S/cm for $LaCr_{0.9}Mg_{0.1}O_3$ and $La_{0.9}Ca_{0.1}CrO_3$, respectively [1]. In spite the fact that the existence of $LaCr_{1-x}Mg_xO_3$ solid solution was known for decades, no systematic studies of its homogeneity range and high-temperature crystal structure and thermal expansion are available to our knowledge.

In the present work we report on homogeneity range, thermal expansion and high-temperature crystal structure of $LaCr_{1-x}Mg_xO_3$, $0.0 < x \leq 0.25$.

* Corresponding author. Tel.: +7 495 9393490, fax: +7 495 9394788.
E-mail address: istomin@icr.chem.msu.ru (S.Ya. Istomin).

0025-5408/$ – see front matter © 2012 Elsevier Ltd. All rights reserved.
doi:10.1016/j.materresbull.2012.02.001

2. Experimental

$LaCr_{1-x}Mg_xO_3$, $0 \le x \le 0.3$ samples were prepared by heating stoichiometric mixtures of La_2O_3, Cr_2O_3 and MgO at 1400 °C for 48 h in air.

Phase purity of the compounds was checked by X-ray powder diffraction (XRPD) recorded in Huber G670 Guinier diffractometer (CuKα1 radiation, image foil detector, Ge-monochromator). Germanium was used as internal standard to determine the unit cell parameters of $LaCr_{1-x}Mg_xO_3$.

High-temperature X-ray powder diffraction (HT XRPD) data for $LaCr_{0.75}Mg_{0.25}O_3$ were collected in air using Bruker D8-Advance diffractometer (CuKα1 radiation, Vantec PSD) in reflection mode equipped with high-temperature camera XRK-900 (Anton Paar) at 25, 150, 250, 300, 400, 500, 600 and 800 °C. Crystal structures of the $LaCr_{1-x}Mg_xO_3$ at different temperatures were refined by Rietveld method using GSAS program package [20].

Netzsch 402C dilatometer operated in air (298–1273 K, 10 K/min) was used for the thermal expansion behavior studies. For this purpose powders were pressed into pellets 8 mm in diameter and 5–5.5 mm height and annealed at 1400 °C.

3. Results

Single-phase samples of $LaCr_{1-x}Mg_xO_3$ were prepared for $x \le 0.25$. The sample with $x = 0.3$ contained together with perovskite phase an admixture of MgO.

XRD patterns of $LaCr_{1-x}Mg_xO_3$, $x \le 0.25$ were fully indexed in orthorhombic unit cell $a \approx \sqrt{2} \times a_{per}$; $b \approx 2 \times a_{per}$; $c \approx \sqrt{2} \times a_{per}$. Unit cell dimensions are given in Table 1, their compositional dependence are presented in Fig. 1a and b.

3.1. High-temperature crystal structure of $LaCr_{0.75}Mg_{0.25}O_3$

The crystal structure of $LaCr_{0.75}Mg_{0.25}O_3$ was refined using high-temperature XRPD data. XRPD patterns at 25, 150 and 250 °C were fully indexed in $GdFeO_3$-type orthorhombic unit cells, while patterns at $T > 400$ °C were indexed in rhombohedral unit cells, space group $R\text{-}3c$. At 300 °C both orthorhombic and rhombohedral phases were observed on XRPD pattern. Temperature dependence of the perovskite subcell parameters for $LaCr_{0.75}Mg_{0.25}O_3$ is given in Fig. 2.

Crystal structures of both low temperature orthorhombic and high-temperature rhombohedral modifications were refined. Initial atomic coordinates for the orthorhombic and rhombohedral phases were taken from the crystal structures of $LaCrO_3$ [12] and $LaCoO_3$ [21], respectively. During the refinement occupancy of the B-cation position by chromium and magnesium was fixed at Cr/Mg = 0.75:0.25. Atomic displacement parameters (ADP) for oxygen atoms were fixed at $U = 0.020$ Å^2 and were not refined. As an example, results of the Rietveld refinement's for $LaCr_{0.75}Mg_{0.25}O_3$ using XRPD data collected at 25 °C and 400 °C are given in Table 2. Observed, calculated and difference between them XRPD profiles at 25 °C and 400 °C are given in Fig. 3a and b, respectively. Selected interatomic distances in $LaCr_{0.75}Mg_{0.25}O_3$ at 25 °C and 400 °C are given in Table 3.

Table 1
Unit cell parameters for $LaCr_{1-x}Mg_xO_3$ ($0.05 \le x \le 0.25$).

Composition (x)	a (Å)	b (Å)	c (Å)
0.05	5.4834(2)	7.764(1)	5.5181(5)
0.1	5.4846(2)	7.764(1)	5.518(1)
0.15	5.4859(1)	7.768(2)	5.5168 (2)
0.20	5.489(1)	7.7707(2)	5.5198(2)
0.25	5.489(1)	7.773(1)	5.5189(5)

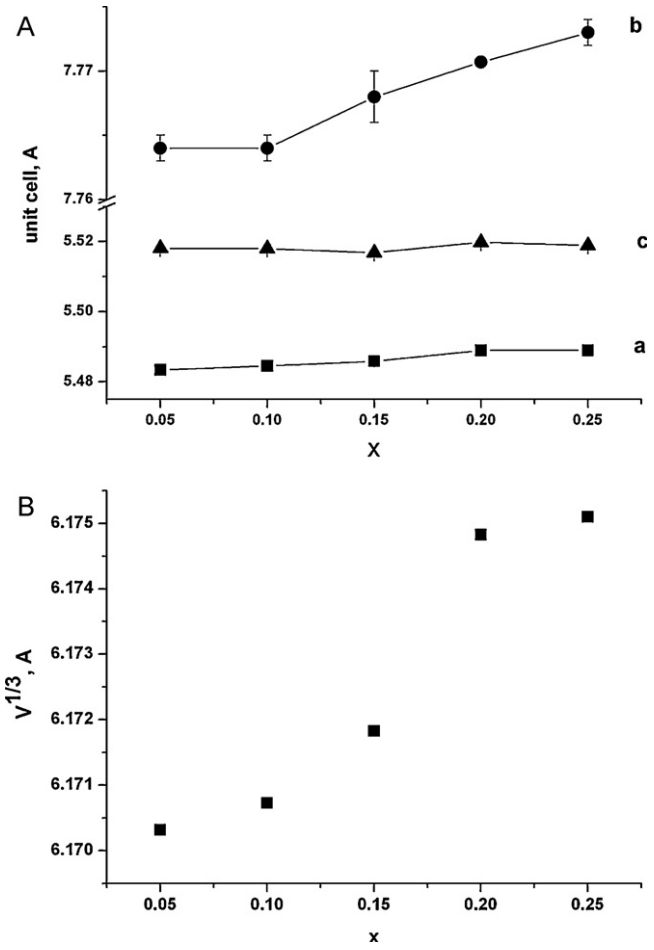

Fig. 1. Unit cell parameters (a) and $V^{1/3}$ (b) versus composition for $LaCr_{1-x}Mg_xO_3$, $0 < x \le 0.25$.

3.2. Thermal expansion properties and phase transition in $LaCr_{1-x}Mg_xO_3$

Thermal expansion curves for $LaCr_{1-x}Mg_xO_3$, $x = 0.0$, 0.05, 0.15 and 0.25 are given in Fig. 4. The kink observed at 250–310 °C on the expansion curves of all compositions corresponds to the first order phase transition from orthorhombic (O) to rhombohedral (R)

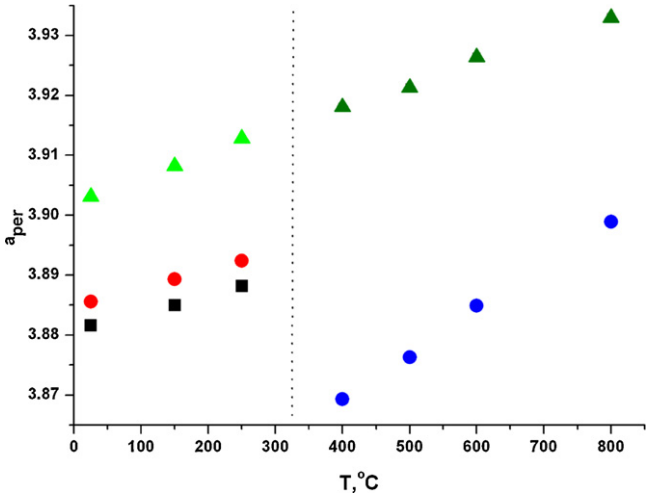

Fig. 2. Temperature dependencies of the perovskite subcell parameters for $LaCr_{0.75}Mg_{0.25}O_3$.

Table 2
Crystal data, atomic coordinates and displacement parameters for $LaCr_{0.75}Mg_{0.25}O_3$ at 25 °C (A) and 400 °C (B).

(A) T = 25 °C				
S.G. *Pnma*, a = 5.4869(1) Å, b = 7.7681(2) Å, c = 5.5177(1) Å; R_{wp} = 0.0337, R_p = 0.0266, χ^2 = 0.918				
Atom	x	y	z	$U_{iso} \times 100$ (Å^2)
La	0.0205(2)	0.25	0.9954(5)	0.87(6)
Cr/Mg[a]	0.5	0.0	0.0	0.83(7)
O1	0.494(2)	0.25	0.062(2)	2.0
O2	0.276(3)	0.029(1)	0.728(2)	2.0
(B) T = 400 °C				
S.G. *R*-3*c*, a = 5.49509(4) Å, α = 60.554°; R_{wp} = 0.0752, R_p = 0.0598, χ^2 = 1.18.				
Atom	x	y	z	$U_{iso} \times 100$ (Å^2)
La	1/4	1/4	1/4	1.83(4)
Cr/Mg[a]	0.0	0.0	0.0	1.11(8)
O1	−0.299(1)	0.799(1)	1/4	1.4(2)

[a] Cr/Mg = 0.75:0.25.

phase. Temperatures of the OR phase transitions (T_{OR}) determined from the dilatometry data are given in Table 4. TECs obtained by linear fit of temperature dependence of $V_{per}^{1/3}$ from high-temperature XRPD data are consistent with those calculated from dilatometry data, see Table 4.

4. Discussion

Charge neutrality requirement leads to two possible scenarios during heterovalent substitution of B-cation in the structure of ABO_3 perovskite by another one (B′) with lower formal oxidation state. In the first case (1) such substitution can lead to the formation of oxygen vacancies according to the formula $AB_{1-x}^{n+}B_x'^{(n-1)+}O_{3-0.5x}$, while in the second one (2) formal oxidation state of the remaining B-cations increases according to the scheme $A(B^{n+})_{1-2x}(B^{n+1})_xB_x'^{(n-1)+}O_3$. Implementation of one of these scenarios is caused by competition between stability of different coordination environments for B-cation and its stability in higher oxidation state. Cr^{3+} ($3d^3$) in oxides is known to be very stable in octahedral coordination. Therefore heterovalent substitution of Cr^{3+} by Mg^{2+} in $LaCrO_3$ leads to the formation of Cr^{4+} (scenario 2) but not oxygen vacancies (scenario 1). Concentration of oxygen vacancies in $La(Cr,Mg)O_3$ perovskites prepared in air is

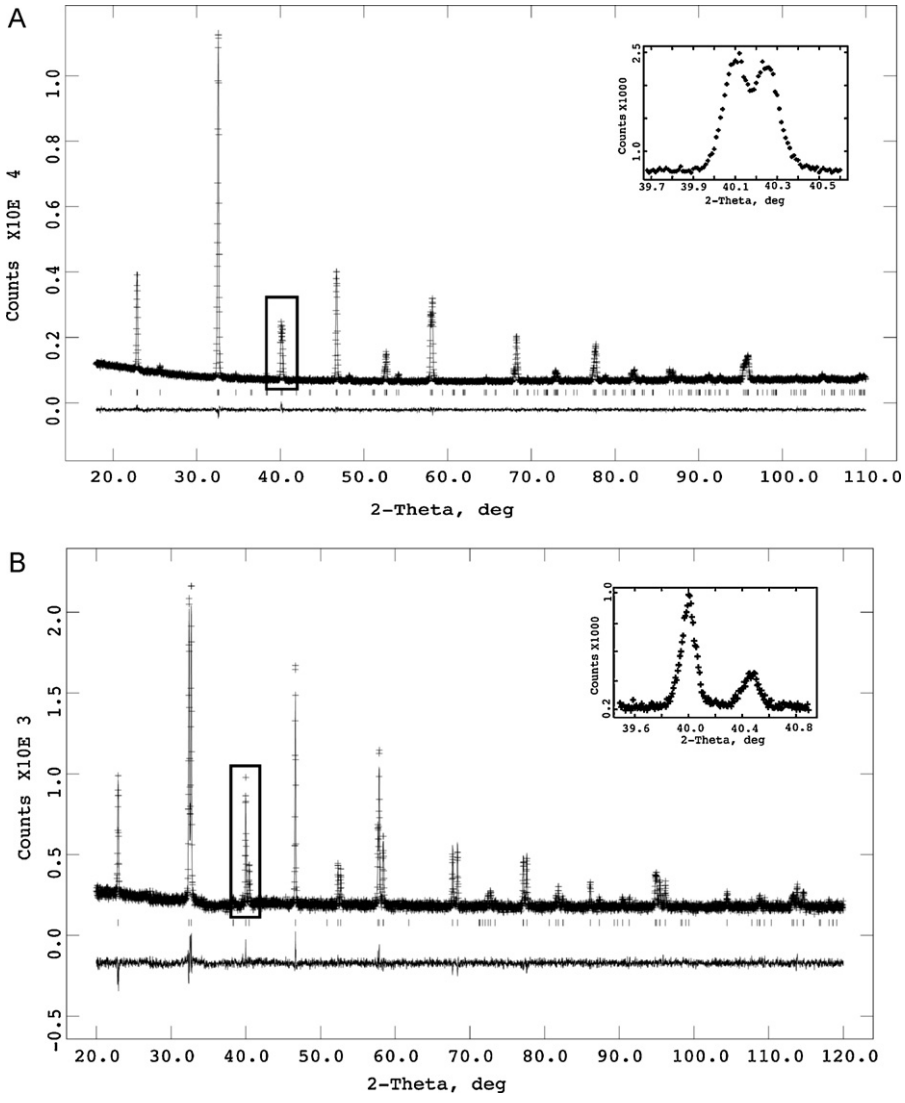

Fig. 3. Observed, calculated and difference between them XRPD profiles for $LaCr_{0.75}Mg_{0.25}O_3$ at 25 °C (A) and 400 °C (B). In the insets split (1 1 1) perovskite subcell reflections are given to emphasize difference in the crystal structure symmetry at 25 °C and 400 °C.

Table 3
Selected interatomic distances (Å) in $LaCr_{0.75}Mg_{0.25}O_3$ at 25 °C (A) and 400 °C (B).

(A) T = 25 °C			
La–O1	2.45(1)	Cr/Mg–O1	1.972(2) × 2
La–O1′	2.62(1)	Cr/Mg–O2	1.95(2) × 2
La–O2	2.505(8) × 2	Cr/Mg–O2′	1.98(2) × 2
La–O2′	2.66(2) × 2	Average: 1.968	
La–O2″	2.75(1) × 2		
Average: 2.613			
(B) T = 400 °C			
La–O1	2.501(8) × 3	Cr/Mg–O1	1.969(1) × 6
La–O1′	2.7607(8) × 6		
Average: 2.674			

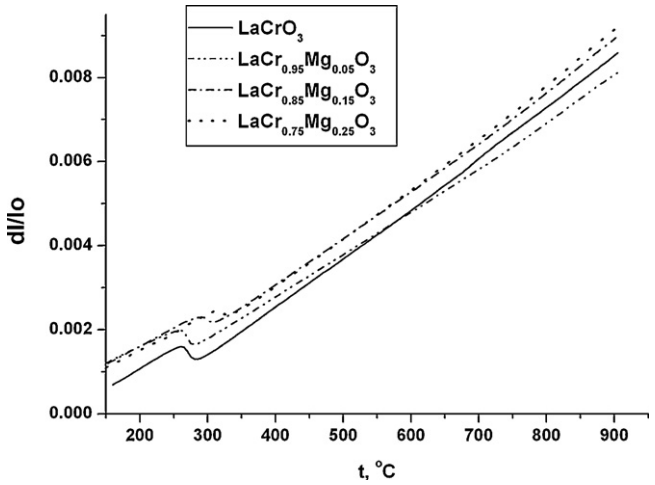

Fig. 4. Thermal expansion curves for $LaCr_{1-x}Mg_xO_3$, x = 0.0, 0.05, 0.15 and 0.25.

very low ($\delta < 0.01$ in $La(Cr,Mg)O_{3-\delta}$ [22]) and only slightly depends on temperature and oxygen partial pressure. According to our data we succeeded to prepare $LaCr_{1-x}Mg_xO_3$ solid solution up to x = 0.25. This corresponds to the formal oxidation state of chromium +3.33. It means that 1/3 of the total amount of chromium is present in the form of Cr^{4+}. Observed narrow homogeneity range for $LaCr_{1-x}Mg_xO_3$ solid solution is most likely due to the large difference in ionic radii of Cr^{3+} and Mg^{2+} ($r(Mg^{2+})$ = 0.72 Å, $r(Cr^{3+})$ = 0.615 Å, CN = 6 [7]) and the instability of Cr^{4+} at the experimental conditions used. At room temperature $LaCr_{1-x}Mg_xO_3$, like $LaCrO_3$, crystallizes in distorted perovskite $GdFeO_3$-type structure with tilt system $a^-b^+a^-$ (*Pnma*) according to Glazer notations [23]. This is due to low tolerance factor (t-factor) which decreases from t = 0.954 for $LaCrO_3$ to t = 0.945 for hypothetical $LaCr_{0.5}Mg_{0.5}O_3$. However, in spite of large difference between ionic radius of Cr^{3+} and Mg^{2+}, unit cell parameters are only slightly dependent on magnesium content (Fig. 1). This is due to the substantial reduction of the average ionic radius of B-cation because of the formation of Cr^{4+} with smaller ionic radius

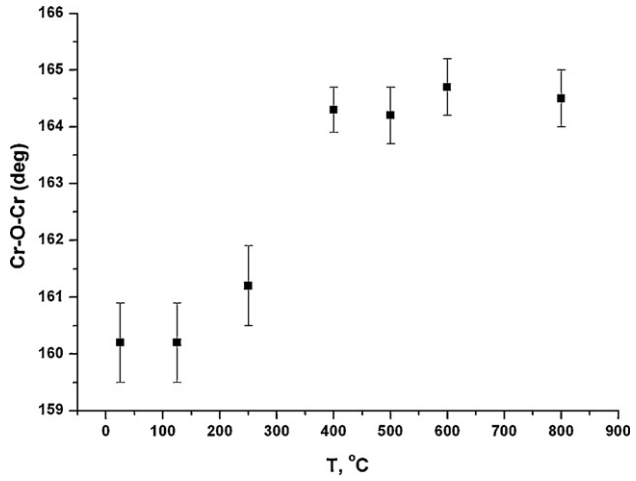

Fig. 5. Temperature variation of (Cr/Mg)–O–(Cr/Mg) bond angle for $LaCr_{0.75}Mg_{0.25}O_3$.

($r(Cr^{4+})$ = 0.55 Å, CN = 6 [7]). For example, average size of B-cation in $LaCr_{0.75}Mg_{0.25}O_3$ is 0.635 Å, which is not significantly higher in comparison with 0.615 Å in $LaCrO_3$. This can partially explain why average (Cr/Mg)–O bond length is comparable (1.968 Å) with that of undoped $LaCrO_3$ (1.972 Å [12]).

From Table 1 it is clear that for all compositions the relationship of the unit cell parameters is $a < c$. According to Zhou and Goodenough [24], such relationship between unit cell parameters is a reason for transition from orthorhombic to rhombohedral phase with tilt system $a^-a^-a^-$ (*R*-3*c*). This happens because for orthorhombic perovskites with large A-cations, BO_6 octahedron becomes strongly distorted in a way that bond angle O–B–O deviates from 90° and this causes shrinking of *a*-axis. The first order phase transitions to *R*-3*c* phase in such distorted orthorhombic perovskite systems occur because the cubic phase cannot be achieved by continuously rotation of the octahedra. $LaCrO_3$ is known to belong to such group of compounds unstable toward OR phase transition. $LaCr_{1-x}Mg_xO_3$ shows OR phase transition at 250–310 °C as evidenced from both high-temperature XRD study and dilatometry. Temperature of OR transition increases gradually with increasing of magnesium content (Table 4). Phase transition is accompanied by a jump of the (Cr/Mg)–O–(Cr/Mg) bond angle (Fig. 5) while (Cr/Mg)–O bond length remains nearly unchanged with increasing temperature from 25 °C (average bond length 1.968 Å) to 400 °C (1.969(1) Å). OR phase transition leads to increase of the coordination number of La^{3+} from 8 in orthorhombic to 9 in rhombohedral phase and to increase of the average La-O bond length from 2.613 to 2.674 Å. Low-temperature orthorhombic phase exhibits TEC lower in comparison with high-temperature rhombohedral one (Table 4). Interestingly, TEC for rhombohedral phase increases with increasing magnesium content. This can be seen from variation of the TEC(R)/TEC(O) ratio which increases gradually from 1.22 for $LaCrO_3$ to 1.39 for $LaCr_{0.75}Mg_{0.25}O_3$. To clarify the nature of this phenomenon additional detailed structural studies are needed.

Table 4
TEC for orthorhombic (O) and rhombohedral (R) modifications of $LaCr_{1-x}Mg_xO_3$, x = 0.0, 0.05, 0.10, 0.15 and 0.25 together with transition temperatures (T_{OR}) obtained from dilatometer data. TEC determined from the temperature dependence of $V_{per}^{1/3}$ are given in parenthesis.

Composition	$LaCrO_3$	$LaCr_{0.95}Mg_{0.05}O_3$	$LaCr_{0.85}Mg_{0.15}O_3$	$LaCr_{0.75}Mg_{0.25}O_3$
TEC(O) (ppm K^{-1})	9.4	8.3 (8.9)	8.8 (7.6)	8.7 (8.5)
TEC(R) (ppm K^{-1})	11.5	10.4 (10.8)	11.6 (12.1)	12.1 (13.0)
TEC(R)/TEC(O)	1.22	1.25	1.32	1.39
T_{OR}	256 °C	260 °C	286 °C	311 °C

Acknowledgments

This work was supported by RFBR (#11-03-01225) and the Ministry of Science and Education of Russian Federation under the State contract 14.740.12.1358.

References

[1] H.U. Anderson, F. Tietz, in: S.C. Singhal, K. Kendall (Eds.), High Temperature Solid Oxide Fuel Cells Fundamentals, Design and Application, Elsevier, 2003, pp. 173–195 (Chapter 7).
[2] R. Berjoan, Rev. Int. Hautes Temp. Refract. 13 (1976) 119.
[3] T. Nakamura, G. Petzow, L.J. Gauckler, Mater. Res. Bull. 14 (1979) 649–659.
[4] T. Hashimoto, N. Tsuzuki, A. Kishi, K. Takagi, K. Tsuda, M. Tanaka, K. Oikawa, T. Kamiyama, K. Yoshida, H. Tagawa, M. Dokiya, Solid State Ionics 132 (2000) 181–188.
[5] K. Oikawa, T. Kamiyama, T. Hashimoto, Y. Shimojyo, Y. Morii, J. Solid State Chem. 154 (2000) 524–529.
[6] H. Tsukuda, Y. Inoue, Y. Uchiyama, J. Ceram. Soc. Jpn. 112 (2004) 167–171.
[7] R.D. Shannon, C.T. Prewitt, Acta Crystallogr. B25 (1969) 925–946.
[8] J. Sfeir, J. van herle, A.J. McEvoy, J. Eur. Ceram. Soc. 19 (1999) 897–902.
[9] J.D. Carter, et al. in: Proceedings of the Third International Symposium on SOFC, The Electrochemical Society Inc., NJ, Honolulu, Hawaii, 1993, pp. 344–353.
[10] D.H Peck, M. Miller, K. Hilpert, Solid State Ionics 123 (1999) 47–57.
[11] J.J. Neumeier, H. Terashita, Phys. Rev. B 70 (2004) 214435.
[12] N. Sakai, H. Fjellvâg, B.C. Hauback, J. Solid State Chem. 121 (1996) 202–213.
[13] C.P. Khattak, D.E. Cox, Mater. Res. Bull. 12 (1977) 463–472.
[14] K. Tezuka, Y. Hinatsu, A. Nakamura, T. Inami, Y. Shimojo, Y. Morii, J. Solid State Chem. 141 (1998) 404–410.
[15] M.D. Mathews, B.R. Ambekar, A.K. Tyagi, Thermochim. Acta 390 (2002) 61–66.
[16] T. Hashimoto, et al. Solid Oxide Fuel Cells, vol. VII, 2001-16, Electrochemical Society, 2001, pp. 820–827 (Proceedings).
[17] Y. Matsunaga, F. Nakamura, H. Takahashi, T. Hashimoto, Solid State Commun. 145 (2008) 502–506.
[18] S.R. Nair, R.D. Purohit, A.K. Tyagi, P.K. Sinha, B.P. Sharma, J. Am. Ceram. Soc. 91 (2008) 88–91.
[19] R. Shukla, J. Manjanna, A.K. Bera, S.M. Yusuf, A.K. Tyagi, Inorg. Chem. 48 (2009) 11691–11696.
[20] A.C. Larson, R.B. Von Dreele, General Structure Analysis System (GSAS), Los Alamos National Laboratory Report LAUR, 2000, pp. 86–748.
[21] G. Thornton, B.C. Tofield, A.W. Hewat, J. Solid State Chem. 61 (1986) 301–307.
[22] H.U. Anderson, M.M. Nasrallah, B.K. Flandermeyer, A.K. Agarwal, J. Solid State Chem. 56 (1985) 325–334.
[23] A.M. Glazer, Acta Cryst. B 28 (1972) 3384–3392.
[24] J.-S. Zhou, J.B. Goodenough, Phys. Rev. Lett. 94 (2005) 065501.